

# Intangible Cultural Heritage Complexes in China: Representation and Restoration of Pigmented Reliefs in Kaiping Diaolou

Qingde Li,<sup>a</sup> Tonghui Sang,<sup>b</sup> Yueqiong Li,<sup>a,\*</sup> Mingce Li,<sup>c</sup> and Qi Sun<sup>d</sup>

Restoration techniques were explored for the patterns, materials, and surface pigments of the pigments decoration art of Kaiping Diaolou and Villages, a world cultural heritage site in southern China. Field investigation was supplemented by scanning electron microscopy, microscopic Raman spectroscopy characterization, colorimetric tests, and tensile tests. Materials and concepts for the restoration of the Kaiping Diaolou pigments were analyzed. Raman spectroscopy was used to characterize the surface pigments display of pigments decorative patterns. The main colors of restoration included green, red, white, and blue. The green color was a mixture of colored copper arsenate minerals. The red color was made of hematite ( $\text{Fe}_2\text{O}_3$ ). White was calcite, and blue was lapis lazuli or synthetic ultramarine. SEM revealed both pigments show similar flake flocculent section morphologies. UV accelerated aging experiments showed that the Ultraviolet absorber and antioxidants effectively inhibited the degradation of the interface matrix. The interface was less prone to cracking. The tension test showed that the bond stress reached a maximum value of 0.193 MPa at a curing temperature of 20 °C under 95% ambient humidity. The results provide strong evidence for pigment restoration in Kaiping Diaolou. This study also provides a scientific reference for the pigment conservation of other architectural decorations from the same historical period.

DOI: 10.15376/biores.18.3.5665-5682

*Keywords:* World cultural heritage site; Pigments decoration art; Restoration techniques; Raman microscopy; Surface pigments; New material

*Contact information:* a: School of Industrial Design and Ceramic Art, Foshan University, Foshan, 528225, China; b: Faculty of Creative Technology and Heritage, Universiti Malaysia Kelantan, Bachok, 16100, Malaysia; c: Visual communication design, Universitas Prima Indonesia, Medan, 20112, Indonesia; d: Department of Economics, Business and Humanities, Universitas Tangerang Raya, Tangerang, 15720, Indah; \*Corresponding author: 313119560@qq.com

## INTRODUCTION

Kaiping Diaolou is a special type of Chinese vernacular architecture. It is located in Kaiping City under the jurisdiction of Jiangmen City, Guangdong Province, China. It is a multi-story tower-style building that integrates defense, housing, and Chinese and Western architectural arts. It was built in the 1920s and 1930s. Kaiping Diaolou Buildings spans 112° 13' to 112° 48' East longitude and 21° 56' to 22° 39' North latitude, northeast even Xinhui City, directly north of Heshan City, southeast near Taishan City, southwest of the Enping city, northwest of the neighboring Xinxing City. Kaiping Diaolou Buildings were distributed in the alluvial plain of Tam River, which is low-lying terrain. The river network is dense. Water disrepair, typhoons, and heavy rains often lead to

flooding. The social order in the region has been chaotic. Therefore, the villagers built towers for flood prevention and to guard against banditry. Its characteristic is a combination of Chinese and Western residential construction. The appearance of the watchtowers, especially the top design, is generally complicated and luxurious, using Western architectural details such as Roman-style colonnades, arches, and terraces, and even the most sacred altar in China can be mixed with Western elements. There is an eagle engraved above the shrine on the third floor. The eagle is the representative of Mexico, where the tower owner lived, and the shrine is just one of the manifestations of Chinese Confucianism. The building incorporated imported materials such as red wool mud, and also used a lot of Western construction techniques in corridors, columns, roofs, windows, doors, *etc.*, such as the beautiful and elegant ancient Roman style, and the exquisite and balanced Gothic style windows that pay attention to strength. The gate exhibits dramatic changes of baroque style pigments, *etc.*

Kaiping Diaolou is known as “a model of overseas Chinese culture” and “a stunning architectural art gallery.” The research results of Han *et al.* (2020) show that the decorative artistic features of pigments in the traditional buildings of Kaiping Diaolou are to make full use of the texture and craftsmanship of the materials for artistic processing. Others studied the pattern characteristics of pigments (Sun *et al.* 2019). Yin *et al.* (2019) and Zhang *et al.* (2020) discussed the construction and heritage protection of Kaiping Diaolou pigments and proposed some protection methods and measures.

Zeng *et al.* (2011) found that the decorative patterns of pigments in Kaiping Diaolou buildings can be roughly divided into four types: plant patterns, animal patterns, text patterns, and geometric patterns. Through field research, Huadong (2013) found that the selection and preference of different styles and themes of the decorative patterns of pigments of Kaiping Diaolou architecture are also different. Their research results have all laid the foundation for carrying out the restoration of the pigments.

The above research on Kaiping Diaolou is still at the level of protection, and it is difficult for Kaiping Diaolou to be better restored and historically reproduced. This article will start with the mixture and study how to use the mixture of colored minerals to repair the damaged buildings of Kaiping Diaolou.

### **The Main Restoration Subjects of Kaiping Diaolou Pigments**

The subject matter of pigments is diverse. These subjects are all expressing a kind of ideology (Fengshan *et al.* 2021), such as “Taking oath in the peach garden” and “Three visits to the thatched cottage” and “defining a hero while warming the wine”, *etc.* Guangdong local craft decoration is characterized by the concept of prosperity of people. This is also a long-standing traditional concept of the Chinese nation. Therefore, pine trees, cranes, dragons and phoenixes are often found in the decorative patterns. They are used to express the idea of good luck and prosperity.

The restoration of pigment decoration focuses on historical or Cantonese opera and other local opera stories and folklore. The Chinese-style “happy” and “wealth” characters, lotus leaves, Chinese knots, money, dragons, phoenix, *etc.* are incorporated. In the decoration of the exterior walls, the western style is also incorporated, absorbing the essence of foreign culture.

### **The Restoration Concept of Kaiping Diaolou Pigments**

The Kaiping Diaolou pigments have great restoration value (Chen *et al.* 2017b; Gao *et al.* 2020). For example, the patterns of wallpaper, furniture, pillows, photo frames,

and curtains show the various flowers, birds, insects, and historical deeds of Kaiping Diaolou's traditional pigments decoration. At the same time, it shows the Chinese characteristics of “happiness” and “Fortune” with the elements of Kaiping Diaolou, and the patterns of lotus leaves, Chinese knots, money, dragons, and phoenixes, which are both personalized. This also reveals a Chinese flavor.

Kaiping Diaolou is a combination of Chinese and Western architecture, and it is also a reflection of regional historical culture in architecture. The blue brick is processed by natural clay and then fired into a blue-black color, which has the characteristics of high density and good frost resistance. It can be researched and developed in building materials to adjust the indoor temperature and humidity to achieve the goal of energy-saving and environmental protection (Chen *et al.* 2017).

The pigments decoration of Kaiping Diaolou buildings is very distinctive, and modern restoration design is also a popular area in recent years. In today's pursuit of personalized decoration, restoration design with Kaiping Diaolou will become a new fashion, and at the same time, traditional Chinese art will also be inherited.

## EXPERIMENTAL

### Architectural Techniques Of Kaiping Diaolou

The architectural style is a combination of Chinese and Western, and is both indigenous and foreign (Kim and Luchkova 2018). There are 1833 existing Diaolou in different styles (Abd Elhady and Abdulghany 2021), none of which are the same (Fig. 1).



**Fig. 1.** Different styles of Diaolou (a) Colonnade style, (b) Castle style, (c) Platform type, (d) Hybrid style

Kaiping Diaolou is a collection of many Western European architectural features, such as the colonnade style of Greece and Rome, the Gothic style of Western Europe, the Italian Baroque style, and the ancient castle style of Europe (Zhong 2020). Kaiping Diaolou

architecture pigments are greatly influenced by Western architectural art and culture and are often used on the facade of the building or the “doors” and “windows” of the buildings (Voss 2018). The shape of the artistic image of the “pigments” on the windows of Kaiping Diaolou buildings can also be flat, triangular, curved, pointed, *etc.* or the deformation of these shapes, *etc.* In addition the objects can be molded with gray or color pigments showing Chinese or Western patterns, such as flowers, melons, fruits, scrolls, and Bogu patterns (Zhu and Eckfeld 2016). In June 28, 2007, the “Kaiping diaolous and ancient villages” application was adopted for the World Heritage project in New Zealand’s 31<sup>st</sup> World Heritage General Assembly. The project was formally included in the “World Heritage List,” becoming China’s 35<sup>th</sup> World Heritage Site. China thus gave birth to the first overseas Chinese culture of the World Heritage project. There is a crisis of destruction of high value of heritage sites today. The surface pigment of the architectural decorative pattern have peeled off. The current solution is to use ancient building restoration techniques. However, researchers face a relative lack of research on the technology of pigment restoration and color restoration, and this study focuses on solving this problem to contribute to the restoration of ancient architectural complexes.

### Micromorphological Analysis

Scanning electron microscopy (SEM) is based on the interaction between electrons and matter. Specifically, when a beam of high-energy incident electrons strikes the surface of a substance, the interaction between the electron and the substance is utilized to obtain a variety of physical and chemical information of each sample. During the test, the material was split into small chunks and the portion facing upward was flattened. It was put on the sample holder, conductive carbon adhesive was applied to both sides of the sample, and the gold film was evaporated and coated using a vacuum coating process. The morphology and characteristics of scanning electronic microlens FEI QUANTA200 (FEI Company, Netherlands) were observed at an accelerated voltage of 15 kV (Kelly 2021).

### Optical Microscopy

Cross sections of the fragments were examined and photographed under white light using a U.S. USCAMEL series microscope (UX002, Orion Optical Instruments Co., Ltd., Guangzhou, China), with a 20× ocular, and a 5× or 10× objective, coupled to a Leica DFC290 digital camera. The layered structures of the cross sections were examined, and the colors of certain pigment grains in the pigment layers were identified. The method characterizes the cross-section of colored fragments. The thickness of the fragments was 200 to 300 μm. The colored fragments were attached directly to the holding table. The cross-sections of the fragments were analyzed by optical microscopy and Raman microscopy.

### Micro-Raman Spectroscopy and Preparation of Pigments Emulsions

Laser Raman Spectroscopy (Finder One, Sanli Technology Co., Ltd., Shenzhen, China) was carried out with a Jobin Yvon LabRam UV-IR HR-800 X-ray fluorescence spectrometer (Finder One, Sanli Technology Co., Ltd., Shenzhen, China) coupled to a U.S. USCAMEL series microscope. Surfaces were lit using either the 488 nm line of an argon-ion laser or the 785 nm line of a near-IR laser diode, with laser power restricted to 1 mW or less. In the Raman shift range of 100 to 2000 cm<sup>-1</sup>, the average spectral resolution was 1 cm<sup>-1</sup> (grating 600 grooves/mm for the laser wavelength 785 nm) and 2 cm<sup>-1</sup> (grating 600 grooves/mm for the laser wavelength 488 nm) (Xue *et al.* 2021). These settings resulted in

spectral imprints with a diameter of 1 to 2 m (50 microscope objectives) on the surfaces of the specimens (Guo and Tang 2015).

The pigments were formulated to the proportions in Table 1. The right amount of water was added to prepare the emulsion. It takes at least 24 h after the defoamer and dispersant have been added to achieve a balance between the durability of the defoaming performance and the shrinkage of holes and edges. Cornish stone, hematite, azurite and synthetic ultramarine were added to color the painted green, red, white and blue respectively. The resulting emulsion can then be used for the restoration of the pigments layer of pigments.

#### UV-accelerated aging test

For the aging test, the sample was placed into a Q-panel UV aging tester (QUV/SPRAY, Q-Panel Company, OH, USA) (Pan 2020; Li *et al.* 2022). According to the aging program based on the ASTM-G-154 standard, the aging process uses a period of 12 h and is divided into two stages (Li *et al.* 2017, 2022). During the first stage, the samples were irradiated under a solar cutoff wavelength of 295 to 365 nm at 0.89W/m<sup>2</sup> irradiance. The chamber was operated under repeated aging cycle conditions of 8 h UV exposure at 60 °C in a dry environment. During the second stage, the samples with the size of 76.2 mm × 76.2 mm × 3 mm were placed in the chamber for aging at 50 °C without UV radiation. After aging for 500, 1000, 1500, 2000, 2500, and 3000 h, the performances of samples were tested and the mean value of five samples was used as the test result.

**Table 1.** The Proportional Composition of Pigments

| Type                    | Element  | Manufacturer                                      | Proportion (%) |
|-------------------------|--|---|----------------|
| Film-forming substances | Resin  | Linhua New Materials Co., Ltd., Guangdong, China  | 30             |
| Extender pigments       | CaCO <sub>3</sub>  | Guangshuo Chemical Co., Ltd., Guangdong, China    | 52             |
| Coloring pigments       | Cornish stone, hematite, azurite and synthetic ultramarine | Hua Dye Chemical Co., Ltd., Shanghai, China       | 10             |
| Solvent                 | 150SN mineral spirits                                      | Hongtai Petrochemical Co., Ltd., Guangdong, China | 2              |
| Antifoaming agent       | Ethylene oxide condensate                                  | Haian Petrochemical Plant, Jiangsu, China         | 2              |
| Ultraviolet absorber    | Tinuvin 770  | Haian Petrochemical Plant, Jiangsu, China         | 1              |
| Antioxidants            | tris(5-tert-butyl-4-hydroxy-o-tolyl)butane                 | Haian Petrochemical Plant, Jiangsu, China         | 1              |
| DPP pigments            | Irgazin® Orange EH 1287                                    | Haian Petrochemical Plant, Jiangsu, China         | 2              |

#### Colorimetric test

The following formula is used for the surface color test:

$$\Delta E^* = (\Delta L^{*2} + \Delta a^{*2} + \Delta b^{*2})^{1/2} \quad (1)$$

$$\Delta L^* = L^* - L_0^* \quad (2)$$

$$\Delta a^* = a^* - a_0^* \quad (3)$$

$$\Delta b^* = b^* - b_0^* \quad (4)$$

The standard for surface color measurement that was used was ASTM D2244. The test tool was a Minolta CR-420 colorimeter (Minolta, Ramsey, New Jersey). The CIELAB system developed by the International Lighting Commission (CIE, 1976) was used for the test. Take  $\Delta L^*$ ,  $\Delta a^*$ , and  $\Delta b^*$  as the difference between the initial and final values of  $L^*$ ,  $a^*$  and  $b^*$ . The  $L^*$  axis represents brightness, the  $a^*$  axis represents red - green coordinates, and the  $b^*$  axis represents yellow - blue coordinates. Three positions were measured for each specimen (Li *et al.* 2017). Test results are based on the average of the four tests.

### Tensile Test

Concrete was used to make the base layer. The ratio of water to cement was 1:2 in the mortar test block. The cement was 42.5 normal silicate cement. The size of the concrete specimen was 70\*70\*20 mm, and after 28 days of curing under standard conditions, a forming frame was placed on top of the concrete specimen and the paint was mixed with water and scraped into the forming frame. After the production, it was put into the curing box with set temperature and humidity (SHBY-40B Concrete Constant Temperature and Humidity Curing Box, Meanyu Instrument Technology Co. After 10 days of curing, tensile test was applied to the specimens by applying tensile testing machine (HS-3000A, 500N universal testing machine, Hesheng Instrument Technology Co., Ltd., Shanghai, China). The experimental standard was performed according to the relevant provisions of "Synthetic resin emulsion sand wall-like architectural coatings" (JG/T24-2000). The ambient temperature was measured in the range of 5 to 40 °C. The ambient humidity was 60, 75 and 95% respectively. The speed of tensile test is 5 mm/min. The tensile and elongation deformation values were automatically recorded by the tester during the tensile test (Peng, K. H., and Tzeng, G. H. 2017).

## RESULTS AND DISCUSSION

### Characterization of Kaiping Diaolou Pigments

According to the visual appearance of the decorative pattern surface of Kaiping Diaolou pigments, the pigments used in pigments is mainly green, red, white, and blue (Fig. 2). The optical microscope image of the pigments on the surface of the Kaiping Diaolou pigments decorative pattern is shown in Fig. 3.



**Fig. 2.** The surface color of the Kaiping Diaolou pigments decoration pattern

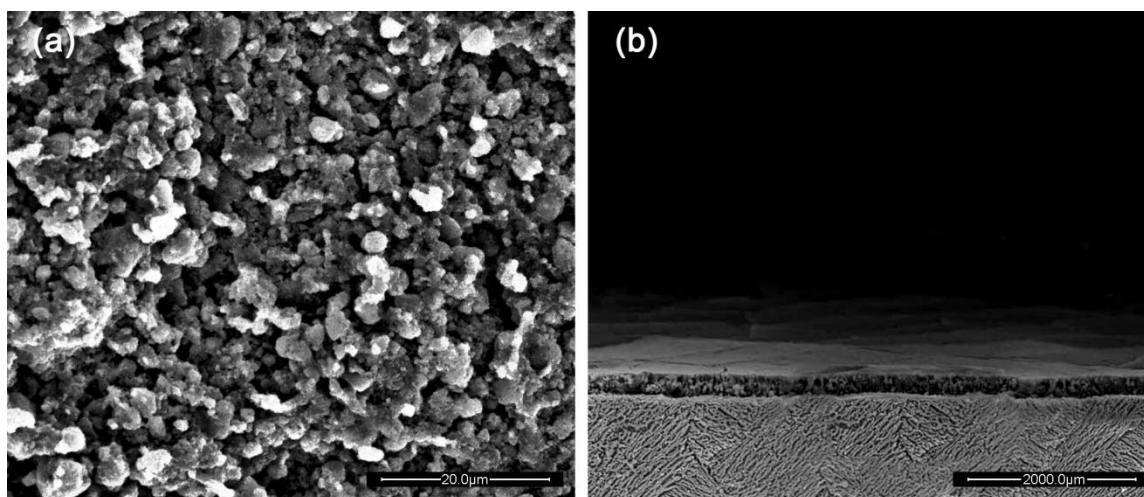


**Fig. 3.** Optical microscope image (a) surface, (b) cross-section

#### *Surface characteristics and analysis of surface pigments of green pigments*

Wavelength Dispersive Laser Raman Spectroscopy showed that the main metal element composition of the green pigments layer on the surface of the Kaiping Diaolou pigments decorative pattern is Pb:Cu:As:Ca=4:5:2:0.25 (molar ratio). According to the database comparison, the green pigments may belong to a mixture of copper arsenate and hard rock minerals, as shown in Figs. 4 (a) and (b). This research result is close to the experimental result of Zeng *et al.* (2010). However, the instrument used previously was a Micro Raman Spectrometer, and the experimental apparatus was different.

The composition of the green pigments layer was further checked by Raman microspectroscopy. The pigments on the surface layer of the green pigments under different excitation wavelengths (785 nm and 488 nm laser lines) are shown in Fig. 4. The peak at approximately  $832\text{ cm}^{-1}$  can be observed in the Raman microscope band at the excitation wavelength (785 nm). This peak appears in Fig. 4 (a). Usually this is attributed to the  $\nu_1(\text{AsO}_4)^{3-}$  (A1) symmetric stretching vibration. This peak may be a mixture of various types of copper arsenate minerals.

Figure 4 (a) shows that when the excitation wavelength was 785 nm, the lead Pb (Pc polycarbonate) molecule exhibited one main absorption spectra in the visible/near the ultraviolet band. The occurrence of strong fluorescence and the self-absorption excitation wavelength in the resonance Raman spectrum will cause the Raman vanishing vibration band. Therefore, the green pigments layer on the surface can be identified as a mixture of corn wollastonite and Pb(Pc).

Figure 4 (b) demonstrates that oscillations were generated when the excitation wavelength was 785 nm. There were  $\nu_2(\text{AsO}_4)^{3-}$  symmetrical and antisymmetrical tensile vibrations at  $862$  and  $819\text{ cm}^{-1}$  of the Raman microspectroscopy. Cu-O stretching vibration and  $\nu_2(\text{AsO}_4)^{3-}$  symmetrical Cornwallite ( $\text{Cu}_5(\text{AsO}_4)_2(\text{OH})_4$ ) bending vibration appeared at  $276\text{ cm}^{-1}$  and  $350\text{ cm}^{-1}$ . From the XRF results, the molar ratio of the two main elements Cu and As is about 5:2. Therefore, the green pigments on the surface layer can be identified as a mixture of Cornish stone. This mixture has not been reported as green pigments in previous literatures.

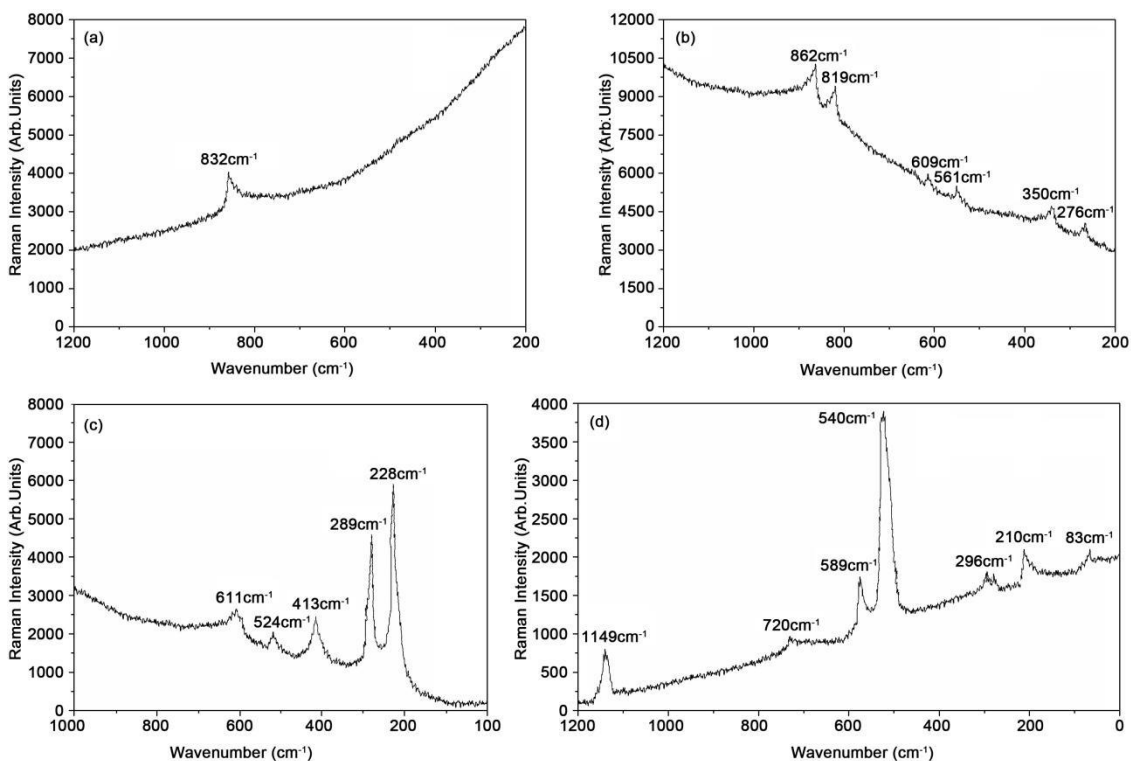


**Fig. 4.** Micro-Raman spectra of the fragment sample (a) the green fragment sample, excitation wavelength (EXC=785nm), (b) excitation wavelength (EXC=448nm), (c) the red fragment sample (EXC=785nm), (d) the blue fragment sample

#### *Surface characteristics and analysis of surface pigments of red pigments*

The optical microscope image of this cross-sectional fragment sample in red is shown in Fig. 4(c). The total thickness of the cross-section was about 300  $\mu\text{m}$ . X-ray fluorescence spectrometer spectral analysis of the cross-section indicated that the ore contained mainly two elements, Fe and Ca, as shown in Fig. 4(a), and was located in the red fragment layer in the “spectrum 4” region of the surface. The Raman bands at 228, 289, 413, 524, and 611  $\text{cm}^{-1}$  indicate hematite ( $\text{Fe}_2\text{O}_3$ ).

Red pigments were present on the surface of the Kaiping Diaolou pigments decorative pattern. These peaks belong to hematite ( $\text{Fe}_2\text{O}_3$ ). This compound is the main component used in pigments. It makes the reliefs colorful. The red color of hematite can resist the damage to the red part of the murals by fog erosion, rain erosion, and weathering erosion in the Lingnan area of China. The red part of the fresco is preserved, so that the whole fresco can be retrospectively restored. It effectively acts as a non-fading color. This allows the cultural characteristics of the Lingnan region to be well expressed (Zheng and Liang 2021).

In Fig. 3 (a), the surface SEM image shows that the red pigments were irregularly granular under the scanning electron microscope at 1300 times. The SEM image on the surface of Fig.3 (b) shows that the cross-section of the red pigments was observed under a scanning electron microscope at 1000 times. The total thickness of the red pigments cross-section was approximately 310 microns. XRF observations showed that these peaks belong to hematite ( $\text{Fe}_2\text{O}_3$ ), as shown in Fig. 4 (c).



### *Surface characteristics and analysis of surface pigments of white and blue pigments*

The micro-Raman spectra of the white and blue regions are given in Fig. 4 (d). There are peaks at 296, 589, and 540  $\text{cm}^{-1}$  in the Raman microscopic band. According to the database comparison, these peaks are celestite or synthetic ultramarine ( $\text{Na}_8(\text{Al}_6\text{Si}_6\text{O}_{24})\text{S}_3$ ). The first two peaks were due to the progression of bending and the symmetrical stretching of  $\text{S}^{2-}$  ions. The last peak was identified as lapis lazuli or synthetic ultramarine  $\text{S}^{2-}$  ion ( $\text{Na}_8(\text{Al}_6\text{Si}_6\text{O}_{24})\text{S}_3$ ), both of which can be used as blue chromophores. For the blue fragment sample, the color had mostly faded and disappeared, leaving only blue particles, as can be observed in Figs. 3 (a) and (b).

There were peaks at 83, 210, 720, and 1149  $\text{cm}^{-1}$  of the Raman microscope band in Fig. 4 (d). According to the database comparison, these peaks are calcite. They can be used as white chromophores. XRF analysis in Fig. 4 (b) (supporting information) indicates that Cr was the dominant element (in addition to Fe) in this layer. The Raman bands at 350, 561, and 609  $\text{cm}^{-1}$  of the green layer in Fig. 4 (b) are characteristic of  $\text{Cr}_2\text{O}_3$ . The bands at 210, 720, and 1149  $\text{cm}^{-1}$  are identified as calcite ( $\text{CaCO}_3$ ) in Fig. 4 (d). For the white layer miscellaneous spots in Fig. 3 (a), the Raman band of calcite is also observed, implying that calcite is the main component of the white layer.

The white and blue areas of the surface of the pigments are mixed, as shown in Fig. 4 (d). These four colors of pigments can be observed in each decorative pattern of Kaiping Diaolou pigments. Through the optical microscope, SEM and micro-Raman spectroscopy experimental methods, the main components of the four pigments applied to the decorative patterns of Kaiping Diaolou pigments can be analyzed during the restoration process. In addition, the weak Raman band at 540  $\text{cm}^{-1}$  in Fig. 4 (d) is assigned to lazurite or synthetic ultramarine, which can be verified from the observation of some small blue patches in the white layer in Fig. 3 (a).

### *Application of various pigments and their influence on wall restoration of Kaiping Diaolou*

The pigments used are mainly green, red, white and blue when restoring pigments. The green pigments can be designated as Cornish stone. The red pigments belong to hematite. The white and blue areas are identified as  $\text{S}^{2-}$  ion ( $\text{Na}_8(\text{Al}_6\text{Si}_6\text{O}_{24})\text{S}_3$ ) of azurite and synthetic ultramarine. The pigments layer of the pigments is exposed to the atmosphere. It is susceptible to wind, sun, salt spray corrosion, precipitation, temperature fluctuations, and other factors. In the function of this external natural environment, the coating layer is susceptible to problems such as cracking, chalking, peeling, and discoloration.

It is important to achieve the original aesthetic maintenance function from the coating. However, the pigments of pigments contain a lot of Cornish stone, hematite, azurite, and synthetic ultramarine and other components. These minerals make the pigments layer have a lot of excellent properties. They can keep the color for a long time. And the decorative properties are also very excellent. They also maintain the original decorative properties for a longer period of time. The coatings are weather-resistant. Therefore, after many years, the pigments layer should not occur these destructive phenomena.

### *Gable decoration restoration*

When the pigments layer was restored, the unrestored part served as a reference (Gao *et al.* 2017, 2018), as shown in Fig. 5 (a). The broken part of the picture was restored,

and the restoration result is shown in Fig. 5 (b). Figure 6 shows the SEM images of the original pigments and the restored pigments on the pigments decoration, respectively (Chen *et al.* 2017a; Xuan *et al.* 2017).



**Fig. 5.** The pigments layer of the Kaiping Diaolou pigments (a) Unrestored, (b) Restored

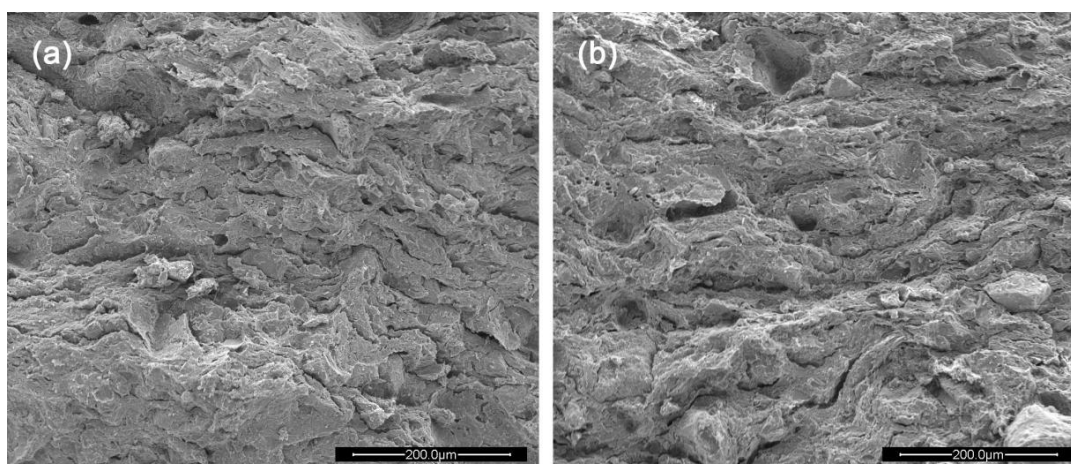


**Fig. 6.** Electron micrographs of the pigments before and after restoration

Figures 6 (a) and (b) show the SEM images of the original pigments and the restored pigments on the pigments decoration, respectively. At the same observation magnification of 200X, both pigments show similar flake flocculent cross-sectional morphologies. These morphologies are composed of chromium minerals and gypsum ( $\text{CaSO}_4 \cdot 2\text{H}_2\text{O}$ ). It is interspersed with Cornish stone, hematite, azurite and synthetic ultramarine particles. The same voids were distributed in the interstices of the flakes' flocculation. This phenomenon indicates that the surface morphology of the pigment specimens before and after the repair matched well when observed at 200X. The uniformity of the particles was very similar. It shows that the repaired pigments layer had the same characteristics as the pigments layer before the restoration. The restoration was thus achieved. The restoration effect was good.

### Effects of UV-Accelerated Aging on Pigment Properties

#### *The surface color of pigments after the UV-accelerated aging*

As demonstrated in Fig. 7 and Table 2, the surface color of pigments varied with the time that samples were exposed to UV-accelerated aging. When the formulated paint

was employed, the changes in luminescence ( $L^*$ ) and color ( $E^*$ ) exhibited comparable patterns. With increasing aging time, the  $L^*$  and  $E^*$  values increased, as did the surface fading. However, the pigments exhibited a little surface fading characteristic due to the UV suppression treatment (Tinuvin 770).  $L^*$  and  $E^*$  exhibited a lesser change for an aging time between 0 and 1000 h; for an aging period between 1000 and 2000 h,  $L^*$  and  $E^*$  grew dramatically and virtually linearly. The  $E^*$  value continued to climb for aging durations greater than 2000 h, although the general trend became smoother.

**Table 2.** The Proportional Composition of Pigments

| Specimen | Exposure time (h) | $\Delta L^*$ (luminescence) | $\Delta E^*$ (color) |
|----------|-------------------|-----------------------------|----------------------|
| 1        | 0                 | 0                           | 0                    |
| 2        | 500               | 5.8                         | 6.2                  |
| 3        | 1000              | 9.1                         | 9.0                  |
| 4        | 1500              | 17.6                        | 18.0                 |
| 5        | 2000              | 20.8                        | 21.1                 |
| 6        | 2500              | 22.2                        | 22.4                 |
| 7        | 3000              | 22.6                        | 23.8                 |

After 3000 h of UV-accelerated aging, the pigments'  $L^*$  and  $E^*$  values were near to 23 and 24, *i.e.* equivalent to the lowest surface color difference. These characterization data demonstrate that under the influence of UV radiation, the pigments' chromophores were momentarily active and then formed a colorless material via oxidation, resulting in the composite's surface fading. The photo-deterioration reaction led to the degradation of the resin in the crystalline areas and an increase in surface brightness. With the addition of an Ultraviolet absorber (Tinuvin 770) and DPP pigments, however, the photodegradation reaction was substantially halted, preserving the surface color.

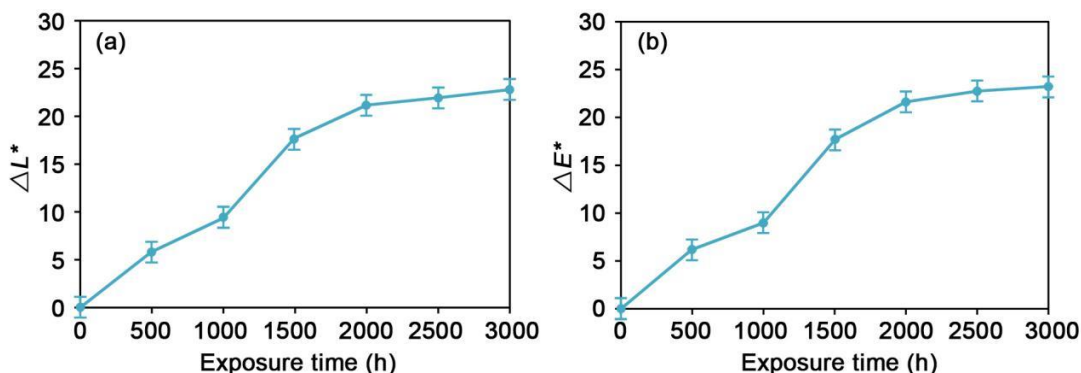


**Fig. 7.** Effect of the duration of UV-accelerated aging treatment on the surface color of pigments (a)  $\Delta L^*$  (luminescence); (b)  $\Delta E^*$  (color)

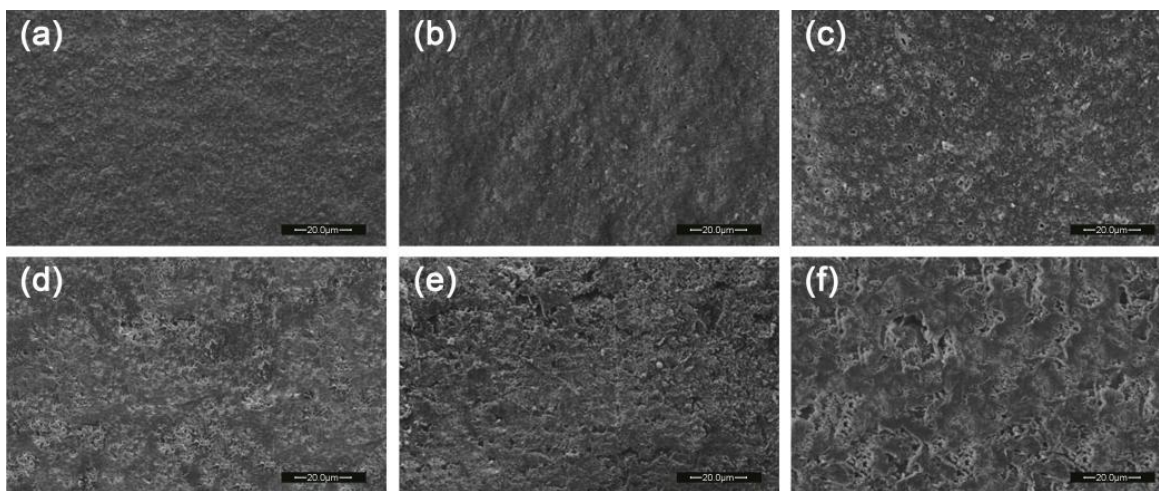
#### *Microstructure and surface morphology of pigments after the UV-accelerated aging*

Figure 8 shows SEM micrographs revealing the surface morphology of the pigments after the UV-accelerated aging. As shown in Fig. 8, after 500 h of UV-accelerated aging, no obvious cracks were found on the surfaces of the samples. For these surfaces, the antioxidants enveloped and protected the resin and  $\text{CaCO}_3$  well, and the DPP pigments samples exhibited the most regular and smooth surfaces. The ultraviolet absorber was uniformly dispersed inside and on the surface of the composite, which further enhanced the anti-aging performance of the composites. After being subjected to 1500 h of UV-

accelerated aging test, the surface of the DPP pigments exhibited smaller cracks as shown in Fig. 8 (c). When the UV accelerated aging test reached 3000 h, the surface of the pigments exhibited the largest cracks as shown in Fig. 8 (f). The ultraviolet absorber to a certain degree blocks the UV light, so that the UV light cannot act directly on the matrix. Instead, it is transformed into heat energy, which then dissipates. This mechanism resulted in a decrease in the degradation rate of the resin and  $\text{CaCO}_3$ , slowed the degradation of the pigments, and led to the generation of some tiny cracks on the surface of the sample, which enhanced the anti-aging performance of the composite.

As demonstrated in Fig. 8 (f), after 3000 h of UV-accelerated aging, the number and size of the surface fractures on the pigments sample increased. However, the surface of the pigments sample exhibited comparatively lesser fissures. The DPP pigments showed better anti-aging performance. This was attributable to the fact that the ultraviolet absorber and antioxidants were able to successfully fill the gaps between the resin and  $\text{CaCO}_3$  matrix, as well as the chemical reaction between components inhibiting the degradation of the interface matrix. Consequently, the interface was less susceptible to breaking. Loss of antioxidants and insufficient wrapping were the primary causes of cracks. It is not possible to efficiently block UV light, exposing the contact between the resin and  $\text{CaCO}_3$ . Under the influence of UV radiation, the exposed region deteriorated to the point that bigger surface fractures appeared.

This phenomenon shows that the degradation of epoxy can be slowed down by adding DPP pigments. Also, the coating's barrier property was improved by increasing the DPP pigments, as shown in Fig. 8. The change of the impedance modulus of each coating formulation as a function of the UV exposure time can demonstrate the influence of UV light on the barrier property of coatings. There is an obvious decrease observed after 3000 h of exposure demonstrating the loss of barrier property caused by UV radiation. This is because most polymers experience more severe degradation at the beginning of UV exposure (Kiil 2012; Zhang *et al.* 2017). The results of the above study suggest that this phenomenon shows that the degradation of epoxy can be slowed down by adding DPP pigments.



**Fig. 8.** Surface morphology of the pigments samples after the UV-accelerated aging (magnification 1000×) (a)500h; (b)1000h; (c)1500h; (d)2000h; (e)2500h; (f)3000h

Also, the coating's barrier property was improved by increasing the DPP pigments, as shown in Fig. 8. The DPP pigments in this study had a platy shape with a particle size of approximately 0.5  $\mu\text{m}$ . Therefore, adding DPP pigments was able to increase the barrier property of epoxy coating. The excellent degradative resistance of the epoxy coating layer was further enhanced. Meanwhile, the DPP pigments can overcome the weakness of the epoxy coating to improve its UV stability. Further tests were done to understand the degradative protection property of coatings. After 3000 h of UV irradiation, the results demonstrate that the coating with higher DPP pigments retained better barrier properties. The trend presented by the results of this experiment is consistent with Zeng's research results (Zeng *et al.* 2018). The one-coat epoxy system with bright orange color, UV stability, and corrosion resistance was developed by incorporating diketopyrrolopyrrole (DPP) into epoxy resins. Coatings with different formulations were exposed in UV aging chamber for different time periods. The UV stabilities of the coatings were evaluated by color difference, gloss retention, and thickness change. Techniques including UV, SEM, and optical microscope were used to characterize the performance of DPP pigments epoxy coatings. However, the UV aging time was 5 days in the cited experiments. Those research findings were not applied to the field of intangible cultural heritage preservation.

### The Influence of Temperature and Humidity on Bonding Strength

Kaiping City is a southern subtropical monsoon maritime climate zone. The annual temperature is between  $-10\text{ }^{\circ}\text{C}$  and  $37\text{ }^{\circ}\text{C}$ . The average annual temperature is 21.5 degrees. The annual rainfall is 1700 to 2400 mm. Therefore, minimum and maximum temperatures of  $5\text{ }^{\circ}\text{C}$  and  $40\text{ }^{\circ}\text{C}$  were selected for the study. The air humidity was set at 60%, 75% and 95%. The relationship between maintenance temperature, humidity and bond strength is shown in Table 3.

**Table 3.** Bond Stress Values for Different Temperature and Humidity Conditions

| Temperature           | Humidity  |           |           |
|-----------------------|-----------|-----------|-----------|
|                       | 60%       | 75%       | 95%       |
| 5 $^{\circ}\text{C}$  | 0.071 MPa | 0.078 MPa | 0.084 MPa |
| 10 $^{\circ}\text{C}$ | 0.094 MPa | 0.102 MPa | 0.139 MPa |
| 15 $^{\circ}\text{C}$ | 0.116MPa  | 0.134 MPa | 0.185 MPa |
| 20 $^{\circ}\text{C}$ | 0.123 MPa | 0.149 MPa | 0.193 MPa |
| 25 $^{\circ}\text{C}$ | 0.114 MPa | 0.131 MPa | 0.175 MPa |
| 30 $^{\circ}\text{C}$ | 0.105 MPa | 0.117 MPa | 0.131 MPa |
| 35 $^{\circ}\text{C}$ | 0.097 MPa | 0.110 MPa | 0.125 MPa |
| 40 $^{\circ}\text{C}$ | 0.085 MPa | 0.102 MPa | 0.117 MPa |

Under the same humidity condition, the bond stress increased significantly when the maintenance temperature was increased from 5 to 20  $^{\circ}\text{C}$ . The bond stress was 0.084 MPa at 5  $^{\circ}\text{C}$  and 0.193 MPa at 20  $^{\circ}\text{C}$  under 95% ambient humidity. Under 95% ambient humidity, the bond stress was 0.084 MPa at 5 $^{\circ}\text{C}$  and 0.193 MPa at 20 $^{\circ}\text{C}$ . The bond stress was increased by 129.8%. This indicates that the maintenance temperature had a large effect on the bond stress. The bond stress decreased when the maintenance temperature was higher than 20  $^{\circ}\text{C}$ . The bond stress of the coating showed the best performance under 95% ambient humidity. The bond stress at 20 $^{\circ}\text{C}$  decreased by 0.062 MPa compared to that at 30 $^{\circ}\text{C}$ .

The maintenance humidity had a large effect on the bond strength. The higher the maintenance humidity at the same temperature, the higher the bond stress, and the

maintenance humidity was almost linearly related to the bond stress. When the ambient humidity was greater than the concrete test block, the moisture in the air entered the interior of the concrete test block along the micro-cracks or pores in the concrete test block. The humidity inside the concrete test block increased. The humidity inside the concrete specimen decreased with the depth gradient. The shrinkage deformation caused by the change in humidity and dryness of the environment was maximum at 25 mm from the surface. The shrinkage deformation caused by wet and dry environment at 50 mm from the surface was the next highest. The part above 200 mm from the surface was less affected by the ambient humidity and could be ignored. The reason for this is that the farther away from the surface, the greater the resistance encountered in the diffusion of internal moisture. It is difficult for the internal moisture to penetrate through the material to the surface. The coating thickness of a paint is usually about 25 mm. This thickness is just in the area most affected by the ambient humidity. The higher the ambient humidity, the more fully hydrated the concrete specimen is. The lower the drying shrinkage deformation. This reduces the number of cracks within the coating and increases the bond stress.

## CONCLUSIONS

1. The restoration of Kaiping Diaolou pigments involves a good fusion of local and foreign cultures. It not only uses local construction techniques, but also uses some new technologies and new materials. The restoration of these patterns in pigments decorative patterns is the main content that should be paid attention to. The main materials for the restoration of pigment decoration are bamboo nails, iron nails, copper wires, tiles, *etc.*, and the technique of restoration is the gray spoon shaping process. The focus of the restoration of pigment decoration is to use history or Cantonese opera and other local opera stories and folklore as themes. Raman spectroscopy is used to characterize the surface pigments display of pigments decorative patterns. The main colors of restoration include green, red, white and blue. Green is a mixture of colored copper arsenate minerals. The red color belongs to hematite ( $\text{Fe}_2\text{O}_3$ ). White is calcite, blue is lapis lazuli or synthetic ultramarine.
2. The pigments emulsion was prepared according to the experimental results. It was then used for the restoration of the pigments layer of pigments. SEM showed that, at the same observation magnification of 200X, both pigments show similar flake flocculent section morphologies. After 3000 h of UV-accelerated aging, the pigments'  $L^*$  and  $E^*$  values were 20.6 and 21.8. These characterization data showed that the photodegradation reaction was largely stopped and the surface color was maintained after the addition of a UV absorber (Tinuvin 770) and DPP pigments.
3. After 3000 h of UV-accelerated aging, the surface fractures of the pigments sample were substantially less. These pigments showed superior anti-aging properties. This was attributable to the fact that the ultraviolet absorber and antioxidants were able to effectively envelop the resin and  $\text{CaCO}_3$  and that the chemical reaction between components inhibited the degradation of the interface matrix. Consequently, the interface is less susceptible to breaking.
4. Under the same humidity condition, the bond stress increased significantly when the maintenance temperature was increased from 5 to 20 °C. At 95% ambient humidity, the

bond stress at 20 °C reached a maximum value of 0.193 MPa, an increase of 129.8%.

5. The results of this research can provide a technical and theoretical basis for the characterization and restoration of the Kaiping Diaolou pigments. It is also able to extend the service life of the pigments layer. It is recommended to use pigments with a high content of Cornish stone, hematite, azurite, synthetic ultramarine, and other components. Compared to common pigments and vegetable pigments. The color of the pigments in the mixture of colored copper arsenate minerals will remain longer. The pigments layer is not prone to cracking, chalking, peeling, and discoloration. Water-based epoxy antirust coatings and UV-curable pigments and their preparation processes were introduced into the next research. These new technologies of environmentally friendly pigments will lead to better restoration of reliefs on the surface of ancient buildings. This material has extremely low release of harmful volatiles. The environmental pollution is greatly reduced.

## ACKNOWLEDGEMENTS

### Funding Statement

This work was supported by The Humanities and Social Science Research Project of the Ministry of Education of China (grant number 20YJC760051) to Prof. Yueqiong Li. Project name: Lingnan traditional architectural decoration research based on the integration of Chinese and Western cultures in the Guangdong-Hong Kong-Macao Greater Bay Area.

### Author Contributions

Qingde Li and Yueqiong Li conceived of and designed the experiments. Qingde Li and Tonghui Sang analyzed and discussed the data. Qingde Li wrote the manuscript, with revisions by Tonghui Sang, Mingce li and Qi Sun.

### Conflicts of Interest

No potential conflict of interest was reported by the authors.

## REFERENCES CITED

- Abd Elhady, S. I., and Abdulghany, R. A. (2021). "Design attributes for a land-based experience of healing-landscaped blue-way system," *African Journal of Biological Sciences* 17(1), 149-169. DOI 10.21608/ajbs.2021.191210
- Chen, F., Han, G., Li, Q., Gao, X., and Cheng, W. (2017a). "High-temperature hot air/silane coupling modification of wood fiber and its effect on properties of wood fiber/HDPE composites," *Materials* 10(3), 286. DOI: 10.3390/ma10030286
- Chen, F., Li, Q., Gao, X., Han, G., and Cheng, W. (2017b). "Impulse-cyclone drying treatment of poplar wood fibers and its effect on composite material's properties," *BioResources* 12(2), 3948-3964. DOI: 10.15376/biores.12.2.3948-3964
- Chen, J. (2017). "The 'biography' of a Buddha image: The transformation of the lore for a stone image of Maitreya in Shicheng," *Studies in Chinese Religions* 3(4), 307-349. DOI: 10.1080/23729988.2018.1429139

- Fengshan, B. I., Yue, L. I., Jingkun, Z. H. A. O., and Nengwei, F. A. N. (2021). "Integrating Chinese culture into English teaching: A case study of Oxford English for junior high schools," *Higher Education of Social Science* 20(2), 69-75. <http://52.196.142.242/index.php/hess/article/view/12250>
- Gao, J., Zhang, C., and Liu, L. (2020). "Communicating the outstanding universal value of World Heritage in China? The tour guides' perspective," *Asia Pacific Journal of Tourism Research* 25(9), 1042-1055. DOI: 10.1080/10941665.2018.1564340
- Gao, X., Li, Q., Cheng, W., Han, G., and Xuan, L. (2017). "High temperature and pressurized steaming/silane coupling co-modification for wood fibers and its effect on the properties of wood fiber/HDPE composites," *Macromolecular Research* 25(2), 141-150. DOI: 10.1007/s13233-017-5024-x
- Gao, X., Li, Q., Cheng, W., Han, G., and Xuan, L. (2018). "Effects of moisture content, wood species, and form of raw materials on fiber morphology and mechanical properties of wood fiber-HDPE composites," *Polymer Composites* 39(9), 3236-3246. DOI: 10.1002/pc.24336
- Guo, C., and Tang, Y. (2015). "Research on principal-agent problem of tourism attractions development: A case study of Kaiping Diaolou," *Journal of Sustainable Development* 8(6), 119-126. DOI 10.5539/jsd.v8n6p119
- Han, W., Cai, J., Wei, Y., Zhang, Y., and Han, Y. (2020). "Impacts of the World Heritage List inscription: A case study of Kaiping Diaolou and villages in China," *Int. J. of Strategic Property Management* 24(1), 51-69. DOI: 10.3846/ijspm.2019.10854
- Huadong, G. (2013). "Kaiping Diaolou and Villages," in: *Atlas of Remote Sensing for World Heritage: China*, Springer, Berlin, pp. 112-117. DOI: 10.1007/978-3-642-32823-7\_15
- Kelly, T. (2021). "The inscription of remnant Things: Zhang Dai's 'Twenty-Eight Friends'," *Late Imperial China* 42(1), 1-43. DOI 10.1353/late.2021.0004
- Kiil, S. (2012). "Model-based analysis of photoinitiated coating degradation under artificial exposure conditions," *Journal of Coatings Technology and Research* 9(4), 375-398. DOI: 10.1007/s11998-011-9383-5
- Kim, A. A., and Luchkova, V. I. (2018). "Assimilation of traditional architecture influenced by the imported styles," *ITU J Faculty Arch* 15, 71-80. DOI: 10.5505/itujfa.2018.32032
- Li, Q., Chen, F., and Sang, T. (2022). "Effects of wood fiber impulse-cyclone drying process on the UV-accelerated aging properties of wood-plastic composites," *PLoS ONE* 17(10): e0266784. DOI: 10.1371/journal.pone.0266784
- Li, Q., Gao, X., Cheng, W., and Han, G. (2017). "Effect of modified red pottery clay on the moisture absorption behavior and weather ability of polyethylene-based wood-plastic composites," *Materials* 10(111), 2-17. DOI: 10.3390/ma10020111
- Li, Q., Gao, X., Cheng, W., Han, G., and Han, J. (2017). "Preparation and performance of high-density polyethylene-based wood-plastic composites reinforced with red pottery clay," *J. Reinf. Plastics Compos.* 36(12), 853-863. DOI: 10.1177/0731684417693698
- Li, Q., Liang, Y., Chen, F., and Sang, T. (2020). "Preparation and performance of modified montmorillonite-reinforced wood-based foamed composites," *BioResources* 15(2), 3566-3584. DOI: 10.15376/biores.15.2.3566-3584
- Pan, L. (2020). "The monument that became public toilet: The New 1st Army Cemetery in Guangzhou," in: *Image, Imagination and Imaginarium*, Palgrave Macmillan, Singapore, pp. 245-313. DOI: 10.1007/978-981-15-9674-2\_5



- Peng, K. H., and Tzeng, G. H. (2017). "Exploring heritage tourism performance improvement for making sustainable development strategies using the hybrid-modified MADM model," *Current Issues in Tourism* 2(4), 1-27. DOI: 10.1080/13683500.2017.1306030
- Sun, J., Zhou, Y., and Wang, X. (2019). "Place construction in the context of world heritage tourism: the case of 'Kaiping Diaolou and Villages'," *Journal of Tourism and Cultural Change* 17(2), 115-131. DOI: 10.1080/14766825.2017.1395441
- Voss, B. L. (2018). "The archaeology of precarious lives: Chinese railroad workers in Nineteenth-Century North America," *Current Anthropology* 59(3), 287-313. DOI: 10.1086/697945
- Voss, B. L., Kennedy, J. R., Tan, J. S., and Ng, L. W. (2018). "The archaeology of home: Qiaoxiang and nonstate actors in the archaeology of the Chinese diaspora," *American Antiquity* 83(3), 407-426. DOI: 10.1017/aaq.2018.16
- Xuan, L., Han, G., Wang, D., Cheng, W., Gao, X., Chen, F., and Li, Q. (2017). "Effect of surface-modified TiO<sub>2</sub> nanoparticles on the anti-ultraviolet aging performance of foamed wheat straw fiber/polypropylene composites," *Materials* 10(5), 456. DOI: 10.3390/ma10050456
- Xue, L., Pan, X., Wang, X., and Zhou, H. (2021). "Lofty buildings towering East and West, Kaiping Watchtower Villages in Central and Southern Guangdong Province," in: *Traditional Chinese Villages*, Springer, Singapore, pp. 45-71. DOI: 10.1007/978-981-33-6154-6\_3
- Yin, J., Tang, X., Zhang, W., Liang, X., and Zhu, J. (2019). "Where to Preserve? Evaluating the integrity principle for delineating protection scopes of Kaiping Diaolou and Villages," *Sustainability* 11(8), 2196. DOI: 10.3390/su11082196
- Zeng, Q. G., Zhang, G. X., Leung, C. W., and Zuo, J. (2010). "Studies of wall painting fragments from Kaiping Diaolou by SEM/EDX, micro Raman and FT-IR spectroscopy," *Microchemical J.* 96(2), 330-336. DOI: 10.1016/j.microc.2010.05.013
- Zeng, Q. G., Zhang, G. X., Tan, J. H., Leung, C. W., and Zuo, J. (2011). "Identification of pigments from the Shrine of Kaiping Diaolou by micro-Raman spectroscopy," *Journal of Raman Spectroscopy* 42(6), 1311-1316. DOI: 10.1002/jrs.2879
- Zeng, W., Zhou, Q., Zhang, H., and Qi, X. (2018). "One-coat epoxy coating development for the improvement of UV stability by DPP pigments," *Dyes and Pigments* 151, 157-164. DOI: 10.1016/j.dyepig.2017.12.058
- Zhang, H., Yang, K., Chen, Y. M., Bhatta, R., Tsige, M., Cheng, S. Z., and Zhu, Y. (2017). "Polymers Based on Benzodipyrrolidone and Naphthodipyrrolidone with Latent Hydrogen-Bonding on the Main Chain," *Macromolecular Chemistry and Physics* 218(13), 1600617. DOI: 10.1002/macp.201600617
- Zhang, L., Yang, S., Wang, D., and Ma, E. (2020). "Perceived value of, and experience with, a World Heritage Site in China—The case of Kaiping Diaolou and villages in China," *Journal of Heritage Tourism* 1-16. DOI: 10.1080/1743873X.2020.1820014
- Zheng, D., and Liang, Z. (2021). "Heterogeneity of residents' dilemmas in supporting sustainable heritage development: An integrated segmentation approach," *Journal of Destination Marketing & Management* 21, article 100635. DOI: 10.1016/j.jdmm.2021.100635
- Zhong, F. (2020, September). "Inheritance and innovative application of Lingnan traditional architectural culture in architectural design," *Journal of Physics: Conference Series* 1649(1), article 012015. IOP Publishing. DOI 10.1088/1742-6596/1649/1/012015

Zhu, Z., and Eckfeld, T. (2016). “The development of conservation practices in China from the 1980s to the present,” *AICCM Bulletin* 37(1), 26-34. DOI: 10.1080/10344233.2016.1206287

Article submitted: April 5, 2023; Peer review completed: May 13, 2023; Revised version received and accepted: June 29, 2023; Published: July 7, 2023.  
DOI: 10.15376/biores.18.3.5665-5682